Inorganic Chemistry
Article
pubs.acs.org/IC

Iron−Bismuth Halido Compounds: Molecules, Clusters, and Polymers

Katarzyna Wójcik,[†] Ana Maria Preda,[†] Lutz Mertens,[†] Petra Ecorchard,[‡] Tobias Rüffer,[‡] Heinrich Lang,[‡] and Michael Mehring*,[†]

[†]Professur Koordinationschemie, Fakultät für Naturwissenschaften, Institut für Chemie, Technische Universität Chemnitz, D-09107 Chemnitz, Germany

[‡]Professur Anorganische Chemie, Fakultät für Naturwissenschaften, Institut für Chemie, Technische Universität Chemnitz, D-09107 Chemnitz, Germany

Supporting Information

ABSTRACT: The pentamethylcyclopentadienyl substituted iron−bismuth halides $[Bi\{FeCp^*(CO)_2\}X_2]$ [X = Cl (**1**), Br (**2**), I (**3**); $Cp^* = \eta^5\text{-}C_5Me_5$] were synthesized starting from $[FeCp^*(CO)_2]_2$ and BiX_3 (X = Cl, Br), followed by halogen exchange reaction with KI in case of **3**. From a reaction mixture of $[FeCp^*(CO)_2]_2$ with $BiCl_3$ in CH_2Cl_2 to which CH_3CN had been added, a novel coordination polymer of the formula $[FeCp^*(CO)_2(CH_3CN)]_{2n}[Bi_4Cl_{14}]_n$ (**4**) was isolated. The change of the molar ratio from 1:1 to 1:2 in the reaction of $[FeCp^*(CO)_2]_2$ with $BiBr_3$ afforded the novel ionic complex $[\{FeCp^*(CO)_2Br\}]_2[Bi_6Br_{22}\{FeCp^*(CO)_2\}]\cdot CH_2Cl_2$ (**5**$\cdot CH_2Cl_2$). It is demonstrated that treatment of $[FeCp^*(CO)_2X]$ (X = Cl, Br) with $BiCl_3$ and $BiBr_3$, respectively, is a more convenient route to synthesize the new halido bismuthates **4** and **5**.

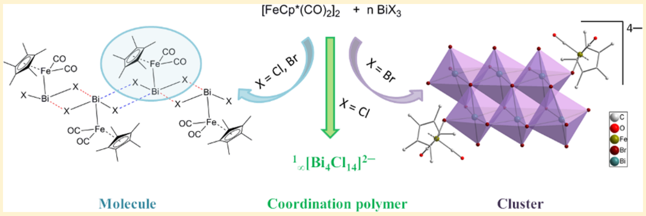

INTRODUCTION

Pentamethylcyclopentadienyl ligands (Cp*) play an important role in transition and main group metal chemistry, especially, because of their steric bulkiness and strongly electron-donating character, which gives access to unusual structures and reactivity, while often providing high solubility.[1,2] For example, this property led to the development of diverse transition metal complexes with high potential in organometallic catalysis.[3−11] With regard to main group metal chemistry, iron carbonyl ligands containing Cp* or its derivatives have gained tremendous interest and have been proven to be versatile in stabilizing various main group metal compounds such as $[Ge\{FeCp^*(CO)_2\}sMes)]$ (sMes = 2,4,6-t-$Bu_3C_6H_3$),[12] $[Ga\{FeCp^*(CO)_2\}(\eta^2\text{-}Cp^*)Cl]$,[13] $[Sn\{FeCp^*(CO)_2\}Cl_3]$,[14] $[(\mu\text{-}E)\{FeCp^*(CO)_2\}_2]^+[BAr^f_4]^-$ [E = Ga, In; Ar^f = 3,5-$(CF_3)_2C_6H_3$],[15] $[Sb\{FeCp^*(CO)_2\}(SiMe_3)_2]$,[16] or $[Bi\{FeCp^*(CO)_2\}_2Cl]_3$.[17]

Within the family of transition metal−bismuth complexes,[1] the $[FeCp(CO)_2]^-$ ligand was introduced to bismuth chemistry first by Cullen in 1971, by the synthesis of $[Bi\{FeCp(CO)_2\}Cl_2]$.[18] The bromide analogue $[Bi\{FeCp(CO)_2\}Br_2]$ was used by Wieber et al. as starting material for the synthesis of the thiocarbamate $[Bi\{FeCp(CO)_2\}(SC(S)NEt_2)_2]$, following an exchange reaction with $NaSC(S)NEt_2$.[19] Other examples of iron−bismuth complexes include $[Bi\{FeCp(CO)_2\}Me_2]$, $[Bi\{Fe(C_5H_4R)(CO)_2\}_2Cl]$ (R = H, Me) and $[Bi\{Fe(C_5H_4R)(CO)_2\}_3]$ (R = H, Me), which were reported by Malisch,[20] Norman,[21] and Schmidbaur,[22] respectively. Later on Gröer and Scheer presented the structure and reactivity of derivatives such as $[Bi\{FeCp^x(CO)_2\}Cl_2]$ [$Cp^x = \eta^5\text{-}C_5H_5$ (Cp), $\eta^5\text{-}C_5H_3{}^tBu_2$ (Cp″)].[23] Although the solubility of compounds with the Cp″ ligand was enhanced as compared to the Cp derivatives, strong intermolecular Bi−Cl interactions were present also in this type of compound, providing coordination polymers of low volatility. Nevertheless, Moniz et al. demonstrated recently that $[Bi\{FeCp(CO)_2\}Cl_2]$ is a potential precursor in the formation of $BiFeO_3$ films via the AACVD method (AACVD = aerosol-assisted chemical vapor deposition).[24] In addition to such bimetallic complexes, polynuclear transition metal main group element clusters were obtained in the reaction of $[Bi\{FeCp^x(CO)_2\}Cl_2]$ (Cp^x = Cp, Cp″) with the transition metalates $K[Co(CO)_4]$ and $Na_2[Fe(CO)_4]$. These reactions led to the formation of bismuth transition metal clusters of the type $[(\mu_3\text{-}Bi)\{Co(CO)_2\}_2\{FeCp(CO)_2\}]$, $[\{Fe_3(CO)_9\}\{\mu\text{-}BiFeCp''(CO)_2\}_2]$ and $[Bi_4\{\mu_3\text{-}Fe(CO)_3\}\{FeCp''(CO)_2\}_2]$.[25] Scheer and co-workers demonstrated that this synthetic strategy offers an interesting opportunity to generate novel transition metal main group clusters of bismuth. In addition to its ability to form metal clusters, bismuth is well-known for the formation of halido clusters as a result of the high Lewis acidity of bismuth halides. Structurally characterized compounds range from dinuclear to polynuclear halobismuthates. Typically, the structures are based on distorted BiX_6-octahedra, whereby association via corners, edges, and faces was described.[26,27] Recently, we have reported on the synthesis and structure of some dinuclear halobismuthates such as $[NnBu_4]_2[\{Bi\{FeCp(CO)_2\}X_3\}_2]$ (X = Cl, Br) and of iron−bismuth complexes

Received: January 15, 2015
Published: March 27, 2015

DOI: 10.1021/acs.inorgchem.5b00088

including [Bi{FeCp^x(CO)$_2$}Br$_2$] [Cp^x = η^5-C$_5$H$_5$ (Cp), η^5-C$_5$H$_3{}^t$Bu$_2$ (Cp″), η^5-C$_5$Me$_5$ (Cp*)].[28] Here, in extension of this work, we present a study on the synthesis of the series [Bi{FeCp*(CO)$_2$}X$_2$] [X = Cl (**1**), Br (**2**), I (**3**)] and report on the formation and structures of the new coordination polymer [FeCp*(CO)$_2$(CH$_3$CN)]$_{2n}$[Bi$_4$Cl$_{14}$]$_n$ (**4**) and the novel heterometallic complex [{FeCp*(CO)$_2$}$_2$Br]$_2$[Bi$_6$Br$_{22}${FeCp*(CO)$_2$}]·CH$_2$Cl$_2$ (**5**·CH$_2$Cl$_2$), the latter showing an unprecedented heterobimetallic halobismuthate cluster.

■ RESULTS AND DISCUSSION

The iron–bismuth compounds [Bi{FeCp*(CO)$_2$}Cl$_2$] (**1**) and [Bi{FeCp*(CO)$_2$}Br$_2$] (**2**) were obtained by the reaction of [FeCp*(CO)$_2$]$_2$ in CH$_2$Cl$_2$ with BiX$_3$ (X = Cl, Br), according to a literature procedure described for **2**,[28] but reaction with BiI$_3$ did not provide the iodide analogue. The IR spectrum obtained for a precipitate did show mainly absorption bands assigned to the starting material [FeCp*(CO)$_2$]$_2$. Thus, [Bi{FeCp*(CO)$_2$}I$_2$] (**3**) was prepared by halogen exchange reaction with KI in acetone starting from **1**, following a procedure adapted from the literature (Scheme 1).[29] Compounds **1**–**3** are highly soluble in CH$_2$Cl$_2$ and THF but show very low solubility in *n*-hexane.

Scheme 1. Synthesis of Compounds 1–3

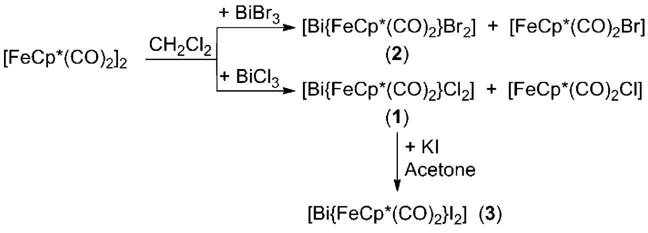

The compounds reveal three absorption bands in the carbonyl region of their IR spectrum at 1997 (s), 1957 (s), 1947 (s) cm^{-1} for **1** and at 1993 (s), 1954 (s), 1946 (s) cm^{-1} for **2**, while only two broad bands (at 1954 (s) and 2006 (s) cm^{-1}) are observed for **3**. The stretching frequencies are slightly blue-shifted, in comparison to those reported for [Bi{FeCp(CO)$_2$}Cl$_2$], [IR/CH$_2$Cl$_2$: 2048 (w), 2016 (s), 1970 (s) cm^{-1}],[30] which probably is a feature of the stronger electron-donating nature of Cp* compared with Cp.[31] Thus, the higher values of stretching wavenumbers for **1**–**3** in comparison to [Bi{FeCp(CO)$_2$}Cl$_2$] indicate the influence of the iron–carbonyl backbonding to be stronger in the Cp* derivatives. A similar influence of the Cp* ligand was observed by Hill et al., who described a series of [{FeCp*(CO)$_2$}R] (R = *n*-C$_3$H$_7$ to *n*-C$_{12}$H$_{25}$) complexes and compared the electronic influence of the Cp* ligand with Cp.[32]

In the ^{1}H NMR spectra of **1**–**3**, a singlet is observed (δ 1.72 (s) for **1**, δ 1.83 (s) for **2**, and δ 1.97 ppm for **3**) that is assigned to the methyl groups of the pentamethylcyclopentadienyl ligand. The increase of the chemical shift correlates with a decrease of the electron-withdrawing effect of the halides. The room-temperature UV-vis spectra of compounds **1**–**3** in the solid state show absorption in the visible-light region and absorption edges were observed at 531 nm for **1**, 652 nm for **2**, and 800 nm for **3** (see Figure S1a in the Supporting Information). Compound **1** shows a structure in the solid state, which is quite close to the previously reported bromide derivative [Bi{FeCp*(CO)$_2$}Br$_2$].[28] Similarly, it is characterized as a one-dimensional coordination polymer resulting from asymmetric intermolecular μ-Cl–Bi coordination. The details of the crystal structure analysis, bond lengths and angles are given in the Supporting Information (Figure S2, Table S1).

Based on a similar protocol as used for the synthesis of [Bi{FeCp*(CO)$_2$}Cl$_2$] (**1**), but using CH$_2$Cl$_2$/CH$_3$CN as solvent, the novel coordination polymer [FeCp*(CO)$_2$(CH$_3$CN)]$_{2n}$[Bi$_4$Cl$_{14}$]$_n$ (**4**) was obtained as a byproduct of **1**. The addition of CH$_3$CN to the CH$_2$Cl$_2$ reaction solution is crucial for the formation of **4** and, after three months of crystallization at 4 °C, a crop of red crystals of **4** was obtained. Most probably, crystallization of **4** instead of **1** results from its lower solubility.

A two-step mechanism for the formation of **4** is assumed (Scheme 2). In the first step, [Bi{FeCp*(CO)$_2$}Cl$_2$] and [FeCp*(CO)$_2$Cl] are formed from [FeCp*(CO)$_2$]$_2$ and BiCl$_3$, followed by the reaction of the very soluble [FeCp*(CO)$_2$Cl] with CH$_3$CN to give [FeCp*(CO)$_2$(CH$_3$CN)]Cl, which reacts with so far unreacted BiCl$_3$. Hereby, the chlorido ligand in [FeCp*(CO)$_2$Cl] is replaced by one molecule of acetonitrile to give [FeCp*(CO)$_2$(CH$_3$CN)]$^+$ and the chloride is trapped by BiCl$_3$ to give the bismuth chlorido complex [Bi$_4$Cl$_{14}$]$_n{}^{2n-}$, finally both crystallizing as [FeCp*(CO)$_2$(CH$_3$CN)]$_{2n}$[Bi$_4$Cl$_{14}$]$_n$ (**4**). Noteworthy, without addition of CH$_3$CN, compound **4** does not form, because of the lack of activation of [FeCp*(CO)$_2$Cl], as confirmed by separate NMR experiments. Thus, it is concluded that [FeCp*(CO)$_2$]$_2$ and [FeCp*(CO)$_2$Cl] are concurring for BiCl$_3$. The proposed mechanism is supported by a separate experiment, starting from a solution of [FeCp*(CO)$_2$Cl] in acetonitrile to which two equivalents of BiCl$_3$ were added at room temperature (eq 2). After 2 days at 4 °C a red precipitate (yield 62%) was obtained, which was identified as complex **4** by IR, UV-vis and NMR spectroscopy, and PXRD analysis (see Figures S3 and S4 in the Supporting Information).

In the IR spectrum of **4**, two strong absorption bands, at 2044 (vs) and 1996 (vs) cm^{-1}, are observed, which are assigned

Scheme 2. Formation of 4 by a Two-Step Process

$$2\,[\mathrm{FeCp^*(CO)_2}]_2 + 2\,\mathrm{BiCl_3} \xrightarrow{\mathrm{CH_2Cl_2}} 2\,[\mathrm{Bi\{FeCp^*(CO)_2\}Cl_2}] + 2\,[\mathrm{FeCp^*(CO)_2Cl}] \qquad \text{(Eq. 1)}$$

$$2\,[\mathrm{FeCp^*(CO)_2Cl}] + 4\,\mathrm{BiCl_3} + 2\,\mathrm{CH_3CN} \xrightarrow{\mathrm{CH_2Cl_2}} [\mathrm{FeCp^*(CO)_2(CH_3CN)}]_{2n}[\mathrm{Bi_4Cl_{14}}]_n\ (\mathbf{4}) \qquad \text{(Eq. 2)}$$

$$[\mathrm{FeCp^*(CO)_2}]_2 + 3\,\mathrm{BiCl_3} + \mathrm{CH_3CN} \xrightarrow{\mathrm{CH_2Cl_2}} \begin{array}{c} 1/2\ [\mathrm{FeCp^*(CO)_2(CH_3CN)}]_{2n}[\mathrm{Bi_4Cl_{14}}]_n\ (\mathbf{4}) \\ + \\ [\mathrm{Bi\{FeCp^*(CO)_2\}Cl_2}] \end{array} \qquad \text{(Eq. 3)}$$

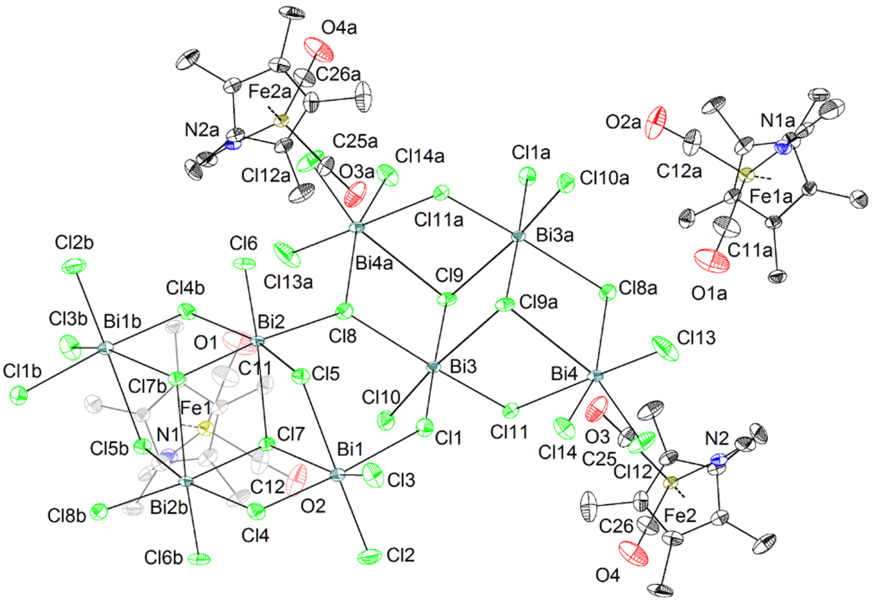

Figure 1. Thermal ellipsoid model of a fragment of the coordination polymer $[FeCp^*(CO)_2(CH_3CN)]_{2n}[Bi_4Cl_{14}]_n$ (**4**). Thermal ellipsoids are set at 50% probability level. Hydrogen atoms are omitted for clarity. Symmetry transformations: $a = 1 - x, 2 - y, -z$, and $b = 1 - x, 2 - y, -1 - z$. Selected bond lengths [Å]: Fe1−D_{Cp^*}, 1.7209(16); Fe2−D_{Cp^*}, 1.7275(15) (D_{Cp^*} = Centroid of the Cp* ring); Bi1−Cl, 2.836(2); Bi1−Cl2, 2.502(2); Bi1−Cl3, 2.4624(19); Bi1−Cl4, 2.623(2); Bi1−Cl5, 3.0490(19); Bi1−Cl7, 3.1117(20); Bi2−Cl5, 2.5473(17); Bi2−Cl6, 2.4635(19); Bi2−Cl7, 3.0877(18); Bi2−Cl8, 2.7614(19); Bi2−Cl14b, 2.9633(18); and Bi2−Cl17b, 2.6903(18). Selected bond angles [°]: Cl1−Bi1−Cl2, 93.22(7); Cl1−Bi1−Cl3, 84.45(7); Cl1−Bi1−Cl4, 173.62(6); Cl1−Bi1−Cl5, 87.24(6); Cl1−Bi1−Cl7, 102.60(5); Cl2−Bi1−Cl3, 94.06(9); Cl2−Bi1−Cl4, 91.98(7); Cl2−Bi1−Cl5, 175.74(7); Cl3−Bi1−Cl4, 91.49(7); Cl3−Bi1−Cl5, 81.76(7); Cl3−Bi1−Cl7, 157.006(7); Cl4−Bi1−Cl5, 87.31(6); Cl5−Bi2−Cl6, 91.58(6); Cl5−Bi2−Cl7, 85.00(5); Cl6−Bi2−Cl7, 173.27(6); Cl6−Bi2−Cl8, 92.66(7); Cl6−Bi2−Cl4b, 89.48(6); Cl6−Bi2−Cl7b, 91.37(6); Cl7−Bi2−Cl8, 93.18(6); Cl7−Bi2−Cl4b, 92.54(5); Cl8−Bi2−Cl5, 90.69(6); Cl8−Bi2−Cl4b, 102.45(6); Cl8−Bi2−Cl7b, 174.67(6).

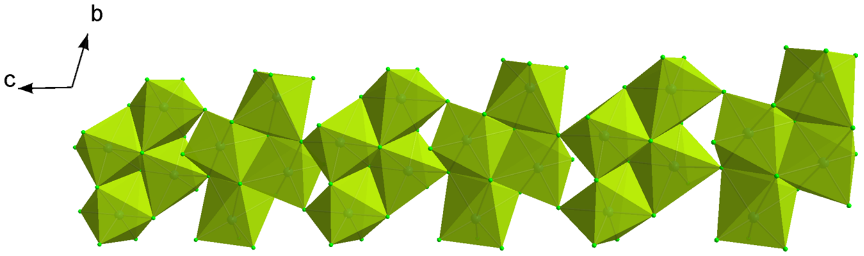

Figure 2. Ball-and-stick representation of the one-dimensional (1D) arrangement of corner-sharing octahedral in units in $^{1}_{\infty}[Bi_4Cl_{14}]^{2-}$.

to the CO groups. The latter differ in position as reported for compounds such as $[Cp^*(CO)_2FeCl]$ (2012 (s), 1967 (s) cm^{-1}),[16] $[Cp^*(CO)_2FeBr]$ (2033 (s), 1978 (s) cm^{-1}),[33] and $[Cp^*(CO)_2Fe(C_5H_{11})]$ (IR/*n*-hexane: 1987 (s), 1933 (s) cm^{-1}),[32] as a result of the ionic character of $[Cp^*(CO)_2Fe(CH_3CN)]^+$. As a consequence, π-back bonding is reduced which results in the stretching wavenumbers shifted to higher values. The ^1H NMR spectrum of complex **4** in DMSO-d_6 shows singlet resonances at δ 1.82 ppm and δ 2.12 ppm, which are assigned to the Cp* ligand and CH_3CN, respectively. In the visible region of the UV-vis spectrum of compound **4**, the absorption edge is observed at 619 nm (see Figure S1b in the Supporting Information).

The complex $[FeCp^*(CO)_2CH_3CN)]_{2n}[Bi_4Cl_{14}]_n$ (**4**) crystallized at 4 °C from CH_2Cl_2/CH_3CN. Selected bond lengths and angles for **4** are listed in Table S2 in the Supporting Information. In the asymmetric unit, two halves of crystallographically independent $[Bi_4Cl_{14}]^{2-}$ units are connected by Bi···Cl interactions with distances in the range of 2.6886(19)−3.173(2) Å (Bi1−Cl1 2.836(2) Å; Bi3−Cl1 2.6886(19) Å; Bi2−Cl8 2.7614(19) Å; Bi3−Cl8 2.9938(19) Å; Bi4a−Cl8 3.173(2) Å (Figure 1). Each anion of the type $^{1}_{\infty}[Bi_4Cl_{14}]^{2-}$ is best described as being composed of four distorted edge-sharing $BiCl_6$ octahedra, which self-assemble to give a 1D coordination polymer (see Figure 2).

Two cations of the type $[FeCp^*(CO)_2(CH_3CN)]^+$ compensate the negative charges and separate the polymer strands in the crystal lattice. The coordination sphere for Bi1 is composed of two terminal and four μ-bridging Cl^- atoms, Bi2 and Bi3 exhibit one terminal and five bridging, whereas Bi4 shows three terminal and three bridging Cl^- atoms. The chlorido ligands in terminal positions show bond lengths in the range $Bi-Cl_{terminal}$ 2.4624(19)−2.502(2) Å and the μ- and μ_3-bridging sites show $Bi-Cl_{bridging}$ distances in the range 2.5466(18)−3.0490(19) and 2.6903(18)−3.0857(19) Å, respectively. These values are in good agreement with those reported for the clusters in $[Et_4N]_6[Bi_8Cl_{30}]$ ($Bi-Cl_{terminal}$ 2.469−2.543 Å, $Bi-Cl_{bridging}$ 2.544−3.207 Å),[34] $[Ph_4P]_4[Bi_4Cl_{16}]\cdot 3CH_3CN$ ($Bi-Cl_{terminal}$ 2.509−2.534 Å, $Bi-Cl_{bridging}$ 2.687−3.045 Å),[35] and $[bpyr]_4[Bi_4Cl_{16}]$ [bpyr = $C_5H_5N(C_4H_9)$] ($Bi-Cl_{terminal}$ 2.509−2.555 Å, $Bi-Cl_{bridging}$ 2.685−3.057 Å).[36] The *cis* Cl−Bi−Cl angles in the octahedra range from 81.76(7)−96.82(5)° and are similar to those reported for $[bpyr]_4[Bi_4Cl_{16}]$ (Cl−Bi−Cl angles 81°−98°).[36] In contrast to $[bpyr]_4[Bi_4Cl_{16}]$ reported by Mahjoor et al.,[36] which, in the crystal lattice, forms only tetramers and separated cations, compound **4** forms a coordination polymer as a result of a different number of chlorido ligands (Figure 2).

In the literature a series of cluster anions, which are composed of assembled $[BiX_6]^{3-}$ octahedra, is reported.[26,27] For example, Zaleski et al. prepared the bismuth chlorido cluster $[Bi_8Cl_{30}]^{6-}$, where the anion is formed by eight edge-sharing octahedra and connected to give a polymeric chain.[34] Four edge-sharing $[BiX_6]^{3-}$ (X = Cl, Br) octahedral units are observed in $[Bi_4Cl_{16}]^{4-}$ [36] and $[Bi_4Br_{16}]^{4-}$.[37] The anion $[Bi_6Br_{22}]^{4-}$ is based on two trimeric units built from six edge-sharing BiX_6 entities[38] and the bismuth iodido cluster $[Bi_4I_{16}]^{4-}$ consists of edge-sharing $[BiI_6]^{3-}$, forming an infinite anionic chain.[39] Recently, Monakhov et al. reported the molecular structure of the first heptanuclear bismuth iodido cluster in $[Bi(OAc)_2(thf)_4]_3[Bi_7I_{24}]$. The structure of the trianion $[Bi_7I_{24}]^{3-}$ is consistent with six edge-sharing BiI_6 moieties arranged in a cyclic manner ($Bi_6(\mu\text{-}I)_6$ ring) through six Bi−(μ-I)−Bi bridges connected to the central BiI_6 octahedron through six μ_3-I ligands (Anderson-type structure).[40] Another example is represented by $[Bi_8I_{28}]^{4-}$, which is composed of polymer strands built up from symmetrical $[Bi_4I_{14}]^{2-}$ fragments joined by edge-sharing octahedra,[41] while compound **4** forms polymeric chains composed of corner-sharing infinite $[Bi_4Cl_{14}]^{2-}$ polyhedra (see Figure 3).

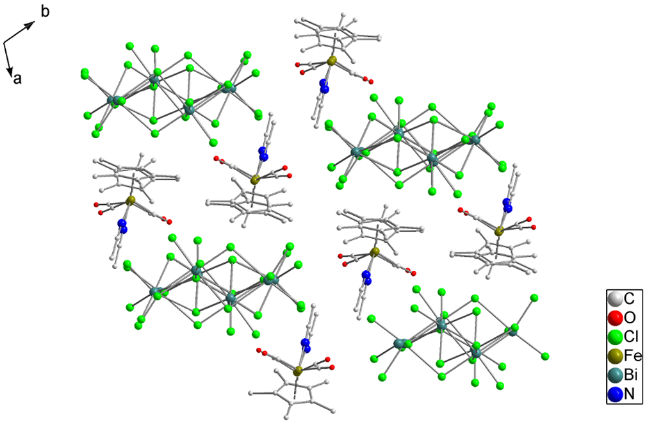

Figure 3. Ball-and-stick model of the packing diagram of compound **4**. Hydrogen atoms are omitted for clarity.

Previously, we have described the synthesis of $[Bi\{FeCp^*(CO)_2\}Br_2]$ (**2**), which was synthesized by the reaction of $[FeCp^*(CO)_2]_2$ with $BiBr_3$ in a 1:1 molar ratio.[28] An unexpected complex was obtained upon changing the molar ratio to 1:2. Red single crystals suitable for X-ray crystallography were isolated upon crystallization from CH_2Cl_2/*n*-hexane at 4 °C, revealing formation of an iron−bismuth cluster of the following composition: $[\{FeCp^*(CO)_2\}_2Br]_2[Bi_6Br_{22}\{FeCp^*(CO)_2\}_2]\cdot CH_2Cl_2$ (**5**·CH_2Cl_2). The IR spectrum shows three strong absorption bands [2031 (s), 1988 (s), 1968 (s) cm^{-1}], which are shifted to higher ν(CO) values in comparison to $[Bi\{FeCp(CO)_2\}Br_2]$ [2008 (s), 1976 (s), 1961 (s) cm^{-1}].[28] The absorption bands are a combination of CO stretching frequencies of cationic $[\{FeCp^*(CO)_2\}_2Br]^+$ [2052 (s), 2009 (s) cm^{-1}][42] and neutral $[FeCp^*(CO)_2Br]$ moieties [2033 (s), 1978 (s) cm^{-1}].[33] However, the ^1H NMR spectrum shows only one singlet at 1.84 ppm for the CH_3 groups, probably due to fast exchange between the $FeCp^*(CO)_2$ fragments in solution.

Formation of **5** is explained by the following steps. First, $[FeCp^*(CO)_2]_2$ and $BiBr_3$ react to give $[Bi\{FeCp^*(CO)_2\}Br_2]$ and $[FeCp^*(CO)_2Br]$, followed by the reaction of the latter molecule with $BiBr_3$ to give $[\{FeCp^*(CO)_2\}_2Br]_2[Bi_6Br_{22}\{FeCp^*(CO)_2\}_2]$ (**5**). This assumption is supported by the following experiment, which is based on a two-step reaction sequence (see Scheme 3). First, the reaction between $[FeCp^*(CO)_2]_2$ and $BiBr_3$ in a 1:1 molar ratio was carried out. After 18 h, an IR spectrum of the solution was measured, which revealed the formation of $[Bi\{FeCp^*(CO)_2\}Br_2]$. A second equivalent of $BiBr_3$ then was added to the red solution and the IR spectrum now was indicative of the formation of **5**. The latter was separated by crystallization from a CH_2Cl_2/*n*-hexane solution at 4 °C. In an additional experiment, compound **5** was independently prepared by the reaction of $[FeCp^*(CO)_2Br]$ with $BiBr_3$ in a 1:1 molar ratio in 64% yield (eq 5) and characterized by IR, UV-vis, and NMR spectroscopy and PXRD analysis (see Figures S5 and S6 in the Supporting Information). In the solid-state UV-vis spectrum, the absorption edge for **5** is observed at 732 nm (see Figure S1b in the Supporting Information).

The asymmetric unit of compound **5**·CH_2Cl_2 consists of two halfs of two crystallographically independent entities of $[\{FeCp^*(CO)_2\}_2Br]_2[Bi_6Br_{22}\{FeCp^*(CO)_2\}_2]$ (**5**) and one molecule of CH_2Cl_2. Only slight differences in bond lengths and angles are observed for the crystallographically independent clusters **5a** and **5b**; thus, only **5a** is discussed. The molecular structure is shown in Figure 4, and selected bond distances and angles are given in Table S3 in the Supporting Information.

Compound **5a** is composed of twice as many $[\{FeCp^*(CO)_2\}_2Br]^+$ cations than anion $[Bi_6Br_{22}\{FeCp^*(CO)_2\}_2]^{2-}$. The latter is best described as being composed of six edge-sharing $BiBr_6$ octahedra to formally give $[Bi_6Br_{22}]^{4-}$, coordinated by two $[FeCp^*(CO)_2]^+$ cations (see Figure 5). The

Scheme 3. Reaction Sequences for the Formation of Compound 5

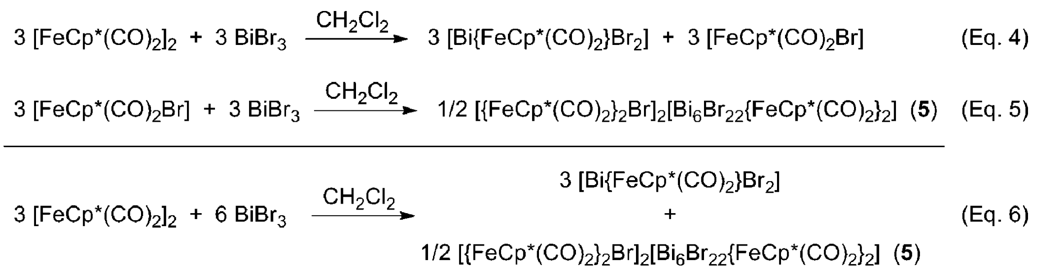

$$3\,[FeCp^*(CO)_2]_2 + 3\,BiBr_3 \xrightarrow{CH_2Cl_2} 3\,[Bi\{FeCp^*(CO)_2\}Br_2] + 3\,[FeCp^*(CO)_2Br] \qquad \text{(Eq. 4)}$$

$$3\,[FeCp^*(CO)_2Br] + 3\,BiBr_3 \xrightarrow{CH_2Cl_2} 1/2\,[\{FeCp^*(CO)_2\}_2Br]_2[Bi_6Br_{22}\{FeCp^*(CO)_2\}_2]\ (\mathbf{5}) \qquad \text{(Eq. 5)}$$

$$3\,[FeCp^*(CO)_2]_2 + 6\,BiBr_3 \xrightarrow{CH_2Cl_2} 3\,[Bi\{FeCp^*(CO)_2\}Br_2] + 1/2\,[\{FeCp^*(CO)_2\}_2Br]_2[Bi_6Br_{22}\{FeCp^*(CO)_2\}_2]\ (\mathbf{5}) \qquad \text{(Eq. 6)}$$

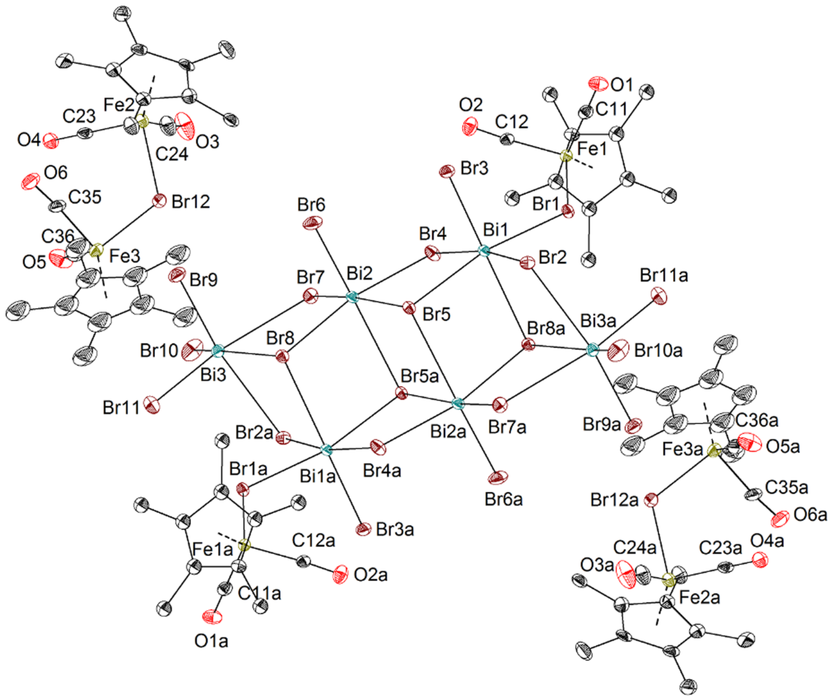

Figure 4. Thermal ellipsoid plot of the molecular structure of $[\{FeCp^*(CO)_2\}_2Br]_2[Bi_6Br_{22}\{FeCp^*(CO)_2\}_2]$ (**5a**). Thermal ellipsoids are set at 30% probability level. Hydrogen atoms were omitted for clarity. Symmetry transformations used to generate equivalent atoms: $a = 1.5 - x, 1.5 - y, 1.5 - z$. Selected bond lengths [Å]: Fe1−D_{Cp*}, 1.7209(16); Fe2−D_{Cp*}, 1.7275(15) (D_{Cp*} = Centroid of the Cp* ring); Fe1−Br1, 2.4325(17); Fe2−Br12, 2.4318(19); Fe3−Br12, 2.434(2); Bi1−Br1, 2.8388(10); Bi1−Br2, 2.7210(10); Bi1−Br3, 2.6414(11); Bi1−Br4, 3.0472(11); Bi1−Br5, 2.9078(10); and Bi1−Br8a, 3.1586(10). Selected bond angles [°]: Fe1−Br1−Bi1, 119.80(5); Fe2−Br12−Fe3, 117.99(7); Br1−Bi1−Br2, 86.88(3); Br1−Bi1−Br3, 94.81(3); Br1−Bi1−Br4, 98.28(3); Br1−Bi1−Br5, 168.81(3); Br1−Bi1−Br8a, 84.36(3); Br2−Bi1−Br3, 93.45(3); Br2−Bi1−Br4, 171.12(3); Br2−Bi1−Br5, 88.33(3); Br2−Bi1−Br8a, 88.51(3); Br3−Bi1−Br4, 93.31(3); Br3−Bi1−Br5, 95.57(3); Br3−Bi1−Br8a, 177.83(3); Br4−Bi1−Br5, 85.29(3); Br4−Bi1−Br8a, 84.83(3); Br5−Bi1−Br8a, 85.41(3).

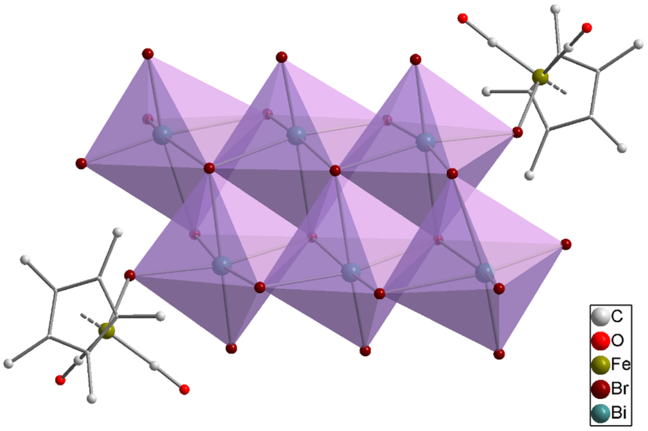

Figure 5. Ball-and-stick model of the molecular structure of the anionic cluster $[Bi_6Br_{22}]^{4-}$ with coordinated $[\{FeCp^*(CO)_2\}_2Br]^+$. The octahedral environment at the Bi atoms is depicted.

coordination sphere for Bi1 consists of one terminal and three μ- and two μ_3-bridging Br atoms; Bi2 shows one terminal, two μ- and three μ_3-bridging Br^- ligands; and Bi3 is coordinated by three terminal, two μ-, and one μ_3-bridging Br atoms. The terminal bond lengths amount to 2.666 Å (average), which is slightly longer than the average value of 2.645 Å for terminal Bi−$Br_{terminal}$ bond lengths, as observed in the isostructural $[Bi_6Br_{22}]^{4-}$ anion, as described by Ahmed and Blachnik.[38] The bridging bonds in **5a** (average length of 2.989 Å) are slightly shorter than reported for $[Bi_6Br_{22}]^{4-}$ (average Bi−$Br_{briging}$ = 3.015 Å).[38] If given separately, the μ- and μ_3-bridging sites show bond distances in the ranges of 2.7069(12)−3.2330(11) Å and 2.8994(11)−3.2382(11) Å, respectively.

The cation $[\{FeCp^*(CO)_2\}_2Br]^+$ can be described to be composed of two $[FeCp^*(CO)_2]^+$ cations bridged by a bromido ligand (see Figure S7 in the Supporting Information). Complexes of this type with the Cp ligand $[\{FeCp(CO)_2\}_2X]^+$ (X = Cl, Br, I), are well-known and were first reported by Fischer et al.[43] For example $[\{FeCp(CO)_2\}_2Br]AlBr_4$ was prepared by reaction of $[FeCp(CO)_2Br]$ with $AlBr_3$ in a 2:1 ratio. Later, it was shown that reactions of $[FeCp(CO)_2X]$ (X = Cl, Br, I) with AgY (Y = BF_4, PF_6) or HPF_6/H_2SO_4 result in compounds of the general type $[\{FeCp(CO)_2\}_2X]Y$.[44,45] In addition, Lorenz et al. previously described several complexes of the formula $[\{FeCp(CO)_2\}_2X]SbY_6$ (X = Cl, Br, I; Y = Cl, F).[42] In $[\{FeCp(CO)_2\}_2Br][SbCl_6]$ Fe−Br distances amount to 2.433(2) Å and 2.413(2) Å. These distances are comparable with those in $[\{FeCp^*(CO)_2\}_2Br]^+$ (Fe2−Br12, 2.432(2) Å; Fe3−Br12, 2.434(2) Å). The Fe−Br−Fe angle Fe2−Br12−Fe3 117.99(7)° in **5a** is slightly larger than the angle Fe−Br−Fe 112.55(6)° in $[\{FeCp(CO)_2\}_2Br][SbCl_6]$, most likely due to packing forces.

■ CONCLUSIONS

Heterometallic bismuth halides of the type $[Bi\{FeCp^*(CO)_2\}X_2]$ [X = Cl (**1**), Br (**2**), I (**3**)] were prepared starting from pentamethylcyclopentadienyl iron derivatives $[FeCp^*(CO)_2]_2$ and bismuth halides BiX_3 (X = Cl, Br). Because of the different reaction conditions, the new one-dimensional (1D) coordination polymer $[FeCp^*(CO)_2(CH_3CN)]_{2n}[Bi_4Cl_{14}]_n$ (**4**) and the heterometallic complex $[\{FeCp^*(CO)_2\}_2Br]_2[Bi_6Br_{22}\{FeCp^*$-

Table 1. Crystallographic Data and Structure Refinement Details for $[Bi\{FeCp^*(CO)_2\}Cl_2]$ (1), $[FeCp^*(CO)_2(CH_3CN)]_{2n}[Bi_4Cl_{14}]_n$ (4), and $[\{FeCp^*(CO)_2\}_2Br]_2[Bi_6Br_{22}\{FeCp^*(CO)_2\}_2]\cdot CH_2Cl_2$ ($5\cdot CH_2Cl_2$)

	1	4	$5\cdot CH_2Cl_2$
empirical formula	$C_{12}H_{15}BiCl_2FeO_2$	$C_{28}H_{36}Bi_4Cl_{14}Fe_2N_2O_4$	$C_{73}H_{92}Bi_6Br_{24}Cl_2Fe_6O_{12}$
M (g mol^{-1})	526.97	1908.51	4739.19
temperature (K)	105	105	100
λ (Å)	0.71073	1.54184	1.54184
crystal system	monoclinic	triclinic	monoclinic
space group	$P2(1)/c$	$P\bar{1}$	$I2/a$
a (Å)	9.1207(2)	12.8907(4)	28.3992(10)
b (Å)	8.8866(2)	15.1214(5)	10.9024(3)
c (Å)	18.7907(5)	15.7675(6)	40.7714(6)
α (deg)	90	99.255(3)	90
β (deg)	94.562(2)	112.110(3)	106.750(3)
γ (deg)	90	106.598(3)	90
V (Å^3)	1518.20(6)	2601.20(15)	12088.0(6)
Z	4	2	4
D_{calc} (g cm^{-3})	2.306	2.437	2.604
μ (Mo Kα) (mm^{-1})	12.873 (Mo Kα)	37.265 (Cu Kα)	32.421 (Cu Kα)
$F(000)$	984	1744	8616
crystal size (mm)	0.3 × 0.3 × 0.2	0.2 × 0.2 × 0.04	0.15 × 0.04 × 0.03
reflections collected	8035	16924	31412
independent reflections	2947	8596	9707
R_{int}	0.0399	0.0335	0.0537
number of data/restraints/parameters	2947/0/163	8596/0/489	9707/164/466
goodness-of-fit on F^2	1.012	1.024	1.036
final R indices $[I > 2\sigma(I)]$			
R_1	0.0292	0.0371	0.0423
wR_2	0.0692	0.0922	0.1117
R indices (all data)			
R_1	0.0385	0.0434	0.0543
wR_2	0.0736	0.0949	0.1212
$\Delta\rho_{min}$ (e Å^{-3})	−1.272	−1.972	−1.847
$\Delta\rho_{max}$ (e Å^{-3})	2.127	2.322	2.894

$(CO)_2\}]\cdot CH_2Cl_2$ ($5\cdot CH_2Cl_2$) showing a unprecedented heterobimetallic halobismuthate cluster were isolated. Both result from the reaction of the formed $[Cp^*(CO)_2FeX]$ (X = Cl, Br), as obtained upon the formation of **1** and **2**, starting from $[FeCp^*(CO)_2]_2$ and BiX_3 (X = Cl, Br), respectively, with excess or unreacted BiX_3. Compounds **4** and **5** are accessible more conveniently by the reaction of separately synthesized $[FeCp^*(CO)_2X]$ with BiX_3. This type of reaction provides access to novel anionic 1D coordination polymers and clusters of the general type $[Bi_nX_m]^{q-}$, which show promising electronic properties, with regard to the development of perovskite-based solar cells.[46] The bismuth−iron halogen complexes **1**−**3** are promising precursors for the synthesis of the multiferroic material $BiFeO_3$, and they might be good starting materials for the formation of novel bismuth−transition metal clusters.

EXPERIMENTAL SECTION

General Procedure. All operations were carried out under dry nitrogen using standard Schlenk techniques. Solvents were freshly distilled over appropriate drying reagents immediately prior to use. The $BiCl_3$ was dried with $SOCl_2$ while $BiBr_3$ was used without further purification. The compounds $[FeCp^*(CO)_2]_2$,[47] $[FeCp^*(CO)_2Br]$,[33] $[FeCp^*(CO)_2Cl]$,[48] and $[Bi\{FeCp^*(CO)_2\}Br_2]$ (**2**)[28] were synthesized corresponding to literature procedures. Infrared spectra with 4 cm^{-1} resolution were recorded on a Nicolet FTIR-200 spectrophotometer as KBr pellet samples. ^1H NMR spectra were recorded with a Bruker Avance 500 (Type Avance III 500) spectrometer at room temperature. The ^1H (500 MHz) chemical shifts are reported in δ units (ppm), relative to the residual peak of the deuterated solvent (ref $CDCl_3$: ^1H 7.26 ppm, DMSO-d_6: ^1H 2.50 ppm). Diffuse reflectance UV-vis spectroscopy was performed using a single-beam simultaneous spectrometer MCS 400 (Carl Zeiss Jena GmbH). The UV and vis radiation were generated using a deuterium lamp CLD 300 and a xenon lamp CLX 11, respectively, at 298 K, using $BaSO_4$ as a reference. The CHN analyses were carried out with a CHN-Analysator FlashAE 1112 (Thermo). Melting points of the compounds were measured with a Melting Point B-540 apparatus (Büchi). PXRD was carried out with a STOE-stad IP device using Cu Kα (λ = 154.184 pm) radiation.

Crystallographic Studies. Crystal data, data collection and refinement parameters for **1**, **4**, and $5\cdot CH_2Cl_2$ are given in Table 1. All data were collected on an Oxford Gemini S diffractometer at 105 K (**1**, **4**), or 100 K ($5\cdot CH_2Cl_2$) using Mo Kα radiation (λ = 0.71073 Å) for **1** or Cu Kα radiation (λ = 1.54184 Å) for **4** and $5\cdot CH_2Cl_2$. For protection against oxygen and moisture, the preparation of the single crystals was performed in perfluoro alkyl ether (ABCR GmbH&Co KG; viscosity 1600 cSt). The structures were solved by direct methods using SHELXS-97[49] and refined by full-matrix least-squares procedures on F2 using SHELXL-97.[49] The drawings were created with the Diamond program.[50] All non-hydrogen atoms were refined anisotropically and a riding model was employed in the refinement of the hydrogen atom positions.

*Synthesis of $[Bi\{FeCp^*(CO)_2\}Cl_2]$ (**1**).* Solid $BiCl_3$ (0.640 g, 2.03 mmol) was added to a vigorously stirred solution of $[FeCp^*(CO)_2]_2$ (1.000 g, 2.03 mmol) in 50 mL of CH_2Cl_2 to give a red-colored solution. After 18 h of stirring, the solvent was reduced to 20 mL and *n*-hexane (20 mL) was added. Crystallization from a mixture of CH_2Cl_2/*n*-hexane at 4 °C gave red crystals of $[Bi\{FeCp^*(CO)_2\}Cl_2]$

(**1**) (0.600 g, 56%) suitable for single-crystal X-ray diffraction (XRD) analysis. Melting point (mp): 150 °C (dec.) ^{1}H NMR (500 MHz, $CDCl_3$): δ 1.72 (s, $C_5(CH_3)_5$). ^{1}H NMR (500 MHz, DMSO-d_6): δ 1.68 (s, $C_5(CH_3)_5$). IR/KBr [ν, cm^{-1}]: 1997 (s); 1957 (vs); 1947 (vs); 1654 (m); 1385 (m); 1261 (m); 1097 (m); 1022 (m); 801 (m); 622(m); 580 (m); 541 (w); 518 (w). Anal. Calcd for $C_{12}H_{15}BiCl_2FeO_2$ (526.98 g/mol): C, 27.35; H, 2.87. Found: C, 27.30; H, 2.70.

Synthesis of [Bi{FeCp(CO)$_2$}I$_2$]* ***(3)***. Solid KI (0.350 g, 2.10 mmol) was added to a solution of [Bi{FeCp*$(CO)_2$}Cl_2] (1) (0.550 g, 1.05 mmol) in 40 mL of acetone at ambient temperature. The color changed to dark brown and the suspension was stirred for 24 h. The solid material was filtered off and the solvent was evaporated in vacuo. [Bi{FeCp*$(CO)_2$}I_2] (**3**) was obtained from a CH_2Cl_2/*n*-hexane solution at 4 °C as brown precipitate (0.320 g, 43%). Melting point (mp): 154 °C (dec.) ^{1}H NMR (500 MHz, $CDCl_3$): δ 1.97 (s, $C_5(CH_3)_5$). IR/KBr [ν, cm^{-1}]: 2964 (m); 2921 (m); 2858 (m); 2006 (s); 1954 (s); 1627 (w); 1409 (m); 1381 (m); 1261 (m); 1095 (m); 1020 (m); 800 (m); 571 (w). Anal. Calcd for $C_{12}H_{15}BiFeI_2O_2$ (709.88 g/mol): C, 20.30; H, 2.13. Found: C, 20.31; H, 2.63.

Synthesis of [FeCp(CO)$_2$(CH$_3$CN)]$_{2n}$[Bi$_4$Cl$_{14}$]$_n$* ***(4)***. Solid $BiCl_3$ (0.313 g, 0.98 mmol) was added in a single portion to a solution of [FeCp*$(CO)_2$Cl] (0.140 g, 0.49 mmol) in 20 mL of acetonitrile at ambient temperature. After 2 days at 4 °C [FeCp*-$(CO)_2(CH_3CN)]_{2n}Bi_4Cl_{14}]_n$ (**4**) was obtained as a red precipitate (0.294 g, 62%). Melting point (mp): 136 °C (dec.) ^{1}H NMR (500 MHz, DMSO-d_6): δ 1.82 [s, 15H, $C_5(CH_3)_5$], 2.12 (s, 3H, CH_3CN). IR/KBr [ν, cm^{-1}]: 2985 (w); 2925 (w); 2044 (vs); 1996 (vs); 1475 (m); 1426 (m); 1384 (m); 1073 (m); 1022 (m); 803 (m); 593 (m); 569 (s); 525 (s); 443 (m). Anal. Calcd for $C_{28}H_{36}Bi_4Cl_{14}Fe_2N_2O_4$ (1908.55 g/mol): C, 17.62; H, 1.90; N, 1.47. Found: C, 17.61; H, 1.72; N, 1.47.

Synthesis of [{FeCp(CO)$_2$}$_2$Br]$_2$[Bi$_6$Br$_{22}${FeCp*(CO)$_2$}$_2$]* ***(5)****, Route A*. Solid $BiBr_3$ (0.800 g, 1.78 mmol) was added to a vigorously stirred solution of [FeCp*$(CO)_2]_2$ (0.440 g, 0.89 mmol) in 40 mL of CH_2Cl_2 to give a dark-red-colored solution. After 18 h of stirring, the solvent was reduced to 20 mL and *n*-hexane was added. After 3 h at 4 °C, red crystals of [{FeCp*$(CO)_2$}$_2$Br]$_2$[Bi_6Br_{22}{FeCp*$(CO)_2$}$_2$] (**5**) (0.450 g, 66%) were formed that were suitable for single-crystal XRD analysis.

Route B. To a solution of [Cp*$(CO)_2$FeBr] (0.500 g, 1.53 mmol) in 20 mL of CH_2Cl_2 was added in a single portion solid $BiBr_3$ (0.690 g, 1.53 mmol). Crystallization at 4 °C from a mixture of the mother liquid to which *n*-hexane was added gave red crystals of **5** (0.740 g, 62%). Melting point (mp): 151 °C (dec.) ^{1}H NMR (500 MHz, $CDCl_3$): δ 1.84 (s, $C_5(CH_3)_5$). IR/KBr [ν, cm^{-1}]: 2963 (w); 2910 (w); 2862 (w); 2031 (s); 1989 (s); 1968 (s); 1617 (m); 1450 (w); 1380 (w); 1262 (m); 1074 (m); 1023 (m); 800 (m); 735 (m); 596 (m); 564 (m); 535 (m). Anal. Calcd for $C_{72}H_{90}Bi_6Br_{24}Fe_6O_{12}$ (4654.13): C, 18.58; H, 1.95. Found: C, 18.98; H, 2.43.

■ ASSOCIATED CONTENT

Ⓢ Supporting Information

UV-vis spectra of solids **1**−**5** (Figures S1a and S1b and PXRD pattern of **4** (Figures S3, S4) and **5** (Figures S5, S6), View of the molecular structures of compound **1**, the cation [{FeCp*-$(CO)_2$}$_2$Br]$^+$ of compound **5**·CH_2Cl_2 (Figures S2, S7) and selected bond distances and angles of compounds **1**, **4**, and **5** (Table S1, S2, and S3). This material is available free of charge via the Internet at http://pubs.acs.org.

■ AUTHOR INFORMATION

Corresponding Author

*Tel.: 49-0-371-531-35128. Fax: 49-0-371-531-21219. E-mail: michael.mehring@chemie.tu-chemnitz.de.

Notes

The authors declare no competing financial interest.

■ ACKNOWLEDGMENTS

We thank Prof. Stefan Spange, for access to diffuse reflectance UV-vis spectroscopy, and Janine Fritzsch, for performing the CHN analyses.

■ DEDICATION

Dedicated to Manfred Scheer on the occasion of his 60th birthday.

■ REFERENCES

(1) Braunschweig, H.; Cogswell, P.; Schwab, K. *Coord. Chem. Rev.* **2011**, *255*, 101.

(2) Theys, R. D.; Dudley, M. E.; Hossain, M. M. *Coord. Chem. Rev.* **2009**, *253*, 180.

(3) Kohl, F. X.; Jutzi, P. *Chem. Ber.* **1987**, *120*, 1539.

(4) (a) Otto, H.; Werner, H. *Chem. Ber.* **1987**, *120*, 97. (b) Jutzi, P.; Schwartzen, K.-H.; Mix, A. *Chem. Ber.* **1990**, *123*, 837.

(5) Burger, U.; Etienne, R. *Helv. Chim. Acta* **1984**, *67*, 2057.

(6) Jutzi, P.; Schwartzen, K.-H.; Mix, A.; Stammler, H. G.; Neumann, B. *Chem. Ber.* **1993**, *126*, 415.

(7) Childs, R. F.; Zeya, M. *J. Am. Chem. Soc.* **1974**, *96*, 6418.

(8) Maeda, H.; Fujiwara, S.; Shin-Ike, T.; Kambe, N.; Sonoda, N. *J. Am. Chem. Soc.* **1996**, *118*, 8160.

(9) Fujiwara, S.; Maeda, H.; Matsuya, T.; Shin-Ike, T.; Kambe, N.; Sonoda, N. *J. Org. Chem.* **2000**, *65*, 5022.

(10) Brune, H. A.; Lach, P.; Schmidtberg, G. *Chem. Ber.* **1985**, *118*, 2671.

(11) Brune, H. A.; Lach, P.; Schmidtberg, G. *Chem. Ber.* **1985**, *118*, 2681.

(12) Jutzi, P.; Leue, C. *Organometallics* **1994**, *13*, 2898.

(13) Jutzi, P.; Neumann, B.; Schebaum, L. O.; Stammler, A.; Stammler, H.-G. *Organometallics* **2000**, *19*, 1445.

(14) Wagner, Ch.; Merzweiler, K. *Z. Anorg. Allg. Chem.* **2002**, *628*, 2241.

(15) Bunn, N. R.; Aldridge, S.; Kays, D. L.; Coombs, N. D.; Rossin, A.; Willock, D. J.; Day, J. K.; Jones, C.; Ooi, L.-l. *Organometallics* **2005**, *24*, 5891.

(16) Weber, L.; Mast, C. A.; Scheffer, M. H.; Schumann, H.; Uthmann, S.; Boese, R.; Bläser, D.; Stammler, H.-G.; Stammler, A. *Z. Anorg. Allg. Chem.* **2000**, *626*, 421.

(17) Clegg, W.; Compton, N. A.; Errington, R. J.; Norman, N. C. *J. Chem. Soc., Dalton Trans.* **1988**, 1671.

(18) Cullen, W. R.; Patmore, D. J.; Sams, J. R.; Newlands, M. J.; Thompson, L. K. *J. Chem. Soc. Chem. Commun.* **1971**, 952.

(19) Wieber, M.; Wirth, D.; Burschka, C. *Z. Naturforsch., B: Anorg. Chem., Org. Chem.* **1985**, *40*, 258.

(20) Kaul, H. A.; Greissinger, D.; Luksza, M.; Malisch, W. *J. Organomet. Chem.* **1982**, *228*, C29.

(21) Clegg, W.; Compton, N. A.; Errington, R. J.; Norman, N. C. *Polyhedron* **1987**, *6*, 2031.

(22) Wallis, J. M.; Mueller, G.; Schmidbaur, H. *J. Organomet. Chem.* **1987**, *325*, 159.

(23) Gröer, T.; Scheer, M. *J. Chem. Soc., Dalton Trans.* **2000**, 647.

(24) Moniz, S. J. A.; Quesada-Cabrera, R.; Blackman, C. S.; Tang, J.; Southern, P.; Weaver, P. M.; Carmalt, C. J. *J. Mater. Chem. A* **2014**, *2*, 2922.

(25) Gröer, T.; Scheer, M. *Organometallics* **2000**, *19*, 3683.

(26) Norman, N. C. In *Chemistry of Arsenic, Antimony and Bismuth*; Godfrey, S. M., McAuliffe, C. A., Mackie, A. G., Pritchard, R. G., Eds.; Blackie Academic and Professional: London, 1998; Chapter 4.2, pp 168−176.

(27) Wu, L.-H.; et al. *Coord. Chem. Rev.* **2009**, *253*, 2787.

(28) Wójcik, K.; Ecorchard, P.; Schaarschmidt, D.; Rüffer, T.; Lang, H.; Mehring, M. *Z. Anorg. Allg. Chem.* **2012**, *638*, 1723.

(29) Dostál, L.; Císařová, I.; Jambor, R.; Růžička, A.; Jirásko, R.; Holeček, J. *Organometallics* **2006**, *25*, 4366.

(30) Cullen, W. R.; Patmore, D. J.; Sams, J. R. *Inorg. Chem.* **1973**, *12*, 867.
(31) Braunschweig, H.; Radacki, K.; Seeler, F.; Whittell, G. R. *Organometallics* **2004**, *23*, 4178.
(32) Hill, R. O.; Marais, C. F.; Moss, J. R.; Naidoo, K. J. *J. Organomet. Chem.* **1999**, *587*, 28.
(33) King, R. B.; Douglas, W. M.; Efraty, A. *J. Orgonomet.Chem.* **1974**, *69*, 131.
(34) Zaleski, J.; Glowiak, T.; Jakubas, R.; Sobczyk, L. *J. Phys. Chem. Solids* **1989**, *50*, 1265.
(35) Ahmed, I. A.; Blachnik, R.; Reuter, H. *Z. Anorg. Allg. Chem.* **2001**, *627*, 2057.
(36) Mahjoor, P.; Latturner, S. E. *Cryst. Growth Des.* **2009**, *9*, 1385.
(37) Rheingold, A. L.; Uhler, A. D.; Landers, A. G. *Inorg. Chem.* **1983**, *22*, 3255.
(38) Ahmed, I. A.; Blachnik, R.; Kastner, G.; Brockner, W. *Z. Anorg. Allg. Chem.* **2001**, *627*, 2261.
(39) Bi, W.; Mercier, N. *Chem. Commun.* **2008**, 5743.
(40) Monakhov, K. Yu.; Gourlaouen, C.; Pattacini, R.; Braunstein, P. *Inorg. Chem.* **2012**, *51*, 1562.
(41) Krautscheid, H. *Z. Anorg. Allg. Chem.* **1995**, *621*, 2049.
(42) Schneider, R.; Lorenz, I.-P.; Nöth, H.; Ponikwar, W. *Z. Anorg. Allg. Chem.* **2001**, *627*, 1775.
(43) Fischer, E. O.; Moser, E. *J. Organomet. Chem.* **1965**, *3*, 16.
(44) Fischer, E. O.; Moser, E. *Z. Anorg. Allg. Chem.* **1966**, *342*, 156.
(45) Symon, D. A.; Waddington, T. C. *J. Chem. Soc., Dalton Trans.* **1974**, 78.
(46) Wang, Y.; Gould, T.; Dobson, J. F.; Zhang, H.; Yang, H.; Yao, Xi.; Zhao, H. *Phys. Chem. Chem. Phys.* **2014**, *16*, 1424.
(47) Barras, J.-P.; Davies, S. G.; Metzler, M. R.; Edwards, A. J.; Humphreys, V. M.; Prout, K. *J. Organomet. Chem.* **1993**, *461*, 157.
(48) Akita, M.; Terada, M.; Tanaka, M.; Morooka, Y. *J. Organomet. Chem.* **1996**, *510*, 255.
(49) Sheldrick, G. M. *Acta Crystallogr., Sect. A: Found. Crystallogr.* **1990**, *46*, 467.
(50) *DIAMOND—Visual Crystal Structure Information System*; Crystal Impact: Bonn, Germany, 2001.